

Hard-axis magnetization of ultrathin Ni(111) films on W(110): An experimental method to measure the magneto-optic Kerr effect in ultrahigh vacuum

M. Farle,* A. Berghaus, Yi Li, and K. Baberschke

Institut für Experimentalphysik, Freie Universität Berlin, Arnimallee 14, D-1000 Berlin 33, Federal Republic of Germany

(Received 7 May 1990; revised manuscript received 20 June 1990)

A setup to measure the magneto-optic Kerr rotation in ultrahigh vacuum from ultrathin ferromagnetic films in magnetic fields of up to 1.4 T is described. Hard-axis-magnetization loops of 10–30-Å thin Ni(111) films are recorded *in situ* with the magnetic field applied normal to the film plane. The anisotropy energy of 10-Å Ni(111) is $\approx -10^6$ erg/cm³ at room temperature, more than 1 order of magnitude larger than in the bulk. Square hysteresis loops are recorded with the field parallel to the film plane. This yields an easy axis of magnetization in the plane oriented along the W(100) direction. The shape of the hard-axis loops depends critically on the perfect alignment of the applied field with respect to the film normal.

The surface magneto-optic Kerr effect (SMOKE) in ultrahigh vacuum has recently been established as a valuable probe to investigate the magnetic properties of ultrathin ferromagnetic films *in situ*. The spontaneous magnetization $\mathbf{M}_{\text{sp}}(T)$ of monolayers and its orientation with respect to the film plane can be detected *in situ* up to the thickness-dependent Curie temperature $T_C(d)$.^{1–4} This demonstrates the high sensitivity of the technique. In the case of Fe monolayers on Ag(100),³ Cu(100), Pd(100), and Ru(0001) (Ref. 4) it has been found that $\mathbf{M}_{\text{sp}}(T)$ is oriented perpendicular to the film plane for certain growth conditions, temperatures, and film thicknesses d . In general, however, the magnetization is found to lie parallel to the film plane, e.g., Ni,³ and Co.⁵ To understand that peculiar behavior of Fe and to compare it to theoretical calculations, one needs to determine the magnetic anisotropy quantitatively, which drives the switching of the magnetization in or out of the plane. For thin films in laboratory air this is routinely done in *ex situ* magneto-optic Kerr effect (MOKE) measurements.^{6,7} Large magnetic fields (> 1 T) can easily be generated under ordinary laboratory conditions and oriented in any direction with respect to the film. If a magnetic field \mathbf{H} is applied and increased along the hard-axis direction, the magnetization rotates out of the easy axis until it is perfectly aligned along the hard axis. The anisotropy field H_{an} is directly given as the applied field \mathbf{H} at which the magnetization is parallel to the hard axis. The magnitude of the necessary field $H = H_{\text{an}}$ to saturate $\mathbf{M}(H, T)$ along the hard axis is estimated from two contributions of \mathbf{H}_{an} : (i) The demagnetization field $H_d = 4\pi(N_{\perp} - N_{\parallel})M(H, T)$ (Ref. 8) of Ni equals 6.4 kG with the saturation magnetization $M(T=0 \text{ K}) = 510$ G. H_d always favors alignment in the film plane. (ii) The magnetocrystalline anisotropy field H_{cryst} (Refs. 9 and 10) is usually smaller and depending on its sign favors a perpendicular orientation or enhances the in-plane orientation of $\mathbf{M}_{\text{sp}}(T)$. For a sample in ultrahigh vacuum (UHV), however, field strengths of a few hundreds gauss have only been generated so far, at most ≈ 3 kG in Ref. 3, and ≈ 1 kG in Ref. 4. This allows the determination of the easy-axis orientation and of the usual small coercive fields H_c along that axis. But H_c is a com-

plicated quantity related to domain-wall nucleation and movement, and contains no information on the out-of-plane anisotropy.

Here we present an experimental setup to measure *in situ* the magneto-optic signal of ferromagnetic monolayers in magnetic fields of up to 1.4 T. The magnetic field can be rotated in a plane normal to the film plane and by a slight modification of the setup also in the film plane. For 10–30-Å thin Ni(111) films on W(110) magnetic hard-axis loops are recorded at room temperature with the magnetic field applied normal to the film plane. From this we determine the anisotropy fields H_{an} and H_{cryst} as function of film thickness.

Our experimental apparatus consists of a conventional UHV chamber equipped with an Auger/low-energy-electron diffraction (LEED) system, sputter gun, and electron-beam-heated evaporation source. At the lower end of the UHV chamber a quartz finger tip (25 mm in diameter) is attached.¹¹ This quartz finger reaches into the pole caps of a 12-in. Varian electromagnet usually employed for ferromagnetic resonance (FMR) and electron paramagnetic resonance (EPR) studies.^{8,11,12} This has the advantage that the magnetic field is created *ex situ* contrary to some other UHV compatible SMOKE setups. Its magnitude is not limited by considerations necessary inside UHV chambers. Depending on the type of pole caps installed, magnetic fields of up to 2.3 T are available. The Kerr effect is detected in the usual way.^{13,14} Linearly polarized light (5 mW HeNe laser) passes through a photoelastic modulator and is reflected from the sample positioned in the quartz tube. The intensity change due to the change in ellipticity and the rotation of the polarization is detected with a linear analyzer and a photodiode. The incident laser light is polarized normal to the scattering plane (s polarized), that is in the film plane. In Fig. 1 we schematically show the two configurations of our experiments. The conventional longitudinal Kerr effect (\mathbf{H} in the film plane and parallel to \mathbf{M}) is depicted in Fig. 1(a). The angle of incidence $\varphi_i \approx 16^\circ$ yields a reduced sensitivity compared to a larger angle, as has been calculated previously,^{15,16} but it is still sensitive enough for Ni monolayers. Figure 1(b) shows our setup for experiments in

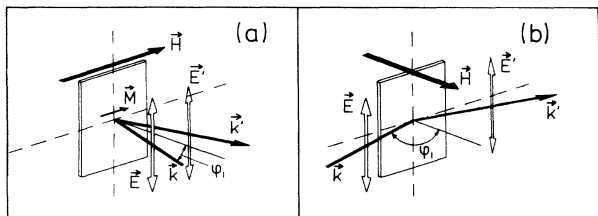


FIG. 1. Schematic of the geometry in our experiments: (a) longitudinal and (b) polar configuration, as discussed in the text. $\mathbf{E}, \mathbf{k}(\mathbf{E}', \mathbf{k}')$ are the electric field and the wave vector of the incident (reflected) light.

UHV. \mathbf{H} is aligned normal ($\phi_h = 90^\circ$) to the film plane. Only in very large fields, that is $H \geq H_{an}$, \mathbf{M} is aligned perpendicular to the film and the polar Kerr effect is observed. For technical reasons we use almost grazing incidence ($\phi_i \approx 74^\circ$). This again is not the best geometry for maximum sensitivity.^{15,16} The quartz finger tip of the UHV chamber, as described in Ref. 11, has obviously the advantage of the use of different geometries for the external magnetic field, the film plane, and the scattering plane of the light. On the other hand, the intensity change detected at the photodiode also contains the Faraday effect of the quartz glass in large fields. Fortunately, this is linear as a function of external field and is subtracted from our experimental data shown in Figs. 2–4. In addition, our present setup makes it very easy to switch between (a) magnetic resonance,¹² (b) ac susceptibility,¹⁷ and (c) magneto-optic measurements on the same sample in UHV. The microwave resonator (a) and the induction coil (b) have central excess holes into which the quartz finger fits.

10–30-Å thin Ni(111) were grown in 10^{-11} Torr ul-

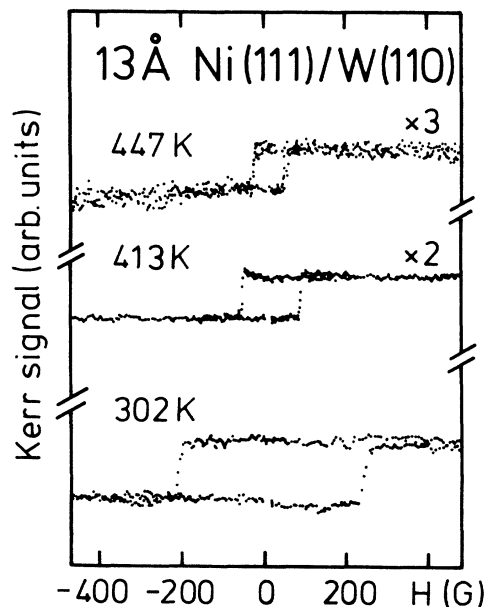


FIG. 2. Longitudinal Kerr signal of 13-Å Ni(111)/W(110) with \mathbf{H} applied in the film plane. Relative gain factors are given. The time constant is reduced at higher T . $H_c(T)$ equals 230, 71, and 41 G.

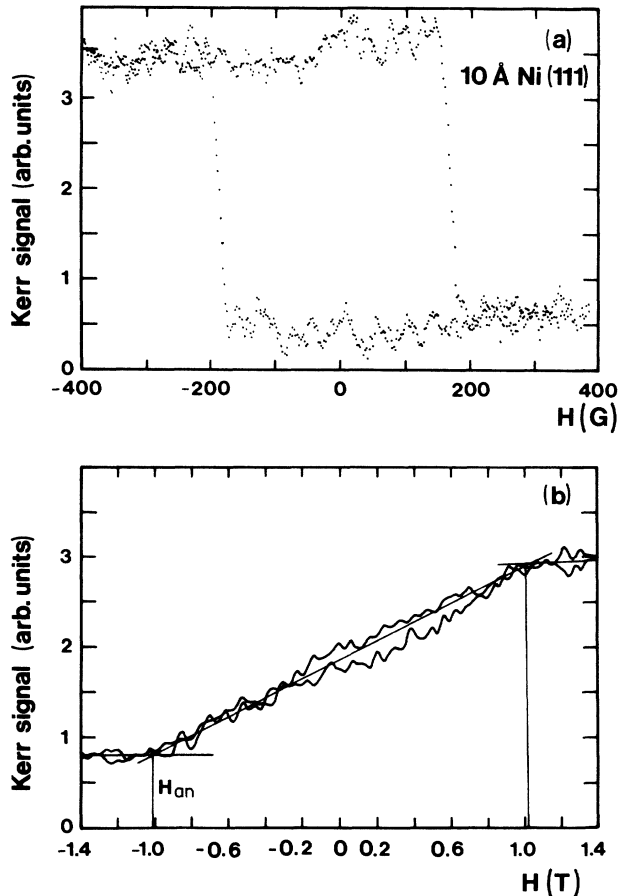


FIG. 3. (a) Hysteresis curve of 10-Å Ni(111) on W(110) at 299 K, as described in the text. $H_c = 190$ G. (b) Magneto-optic signal of the same film, recorded with \mathbf{H} applied normal to the film plane ($\phi_h = 90^\circ$). $H_{an} = 1.03 \pm 0.05$ T.

trahigh vacuum and characterized by LEED and Auger spectroscopy as described earlier.¹² The films grow layer by layer with a nominal layer thickness of $d = 2.035$ Å.

In Figs. 2 and 3(a) we show square hysteresis loops of 13- and 10-Å Ni(111) on W(110). The magnetic field is applied in the film plane along the W(100) direction. As one expects from the temperature-dependent magnetization, the signal height and the coercive field H_c decrease with increasing temperature (Fig. 2). The temperature dependence of these easy-axis SMOKE signals had been analyzed previously for Ni on Cu(100) and Ag(100).³ Here we will not focus on this in detail. The high accuracy in the proportionality between the complex Kerr rotation $\Delta\rho_s$ and the magnetization $M_{sp}(T)$ necessary for a precise analysis is not guaranteed in our setup at present. But a rough estimate from Fig. 2 yields $T_c \geq 460$ K.

The sensitivity of our apparatus is estimated from Fig. 3(a). The hysteresis loop of five atomic layers Ni(111) (10 Å) yields a Kerr signal-to-noise ratio $S/N \approx 8$ at $T/T_c = 0.68$, T_c (10 Å) ≈ 440 K.¹⁸ Using the known temperature dependence of the magnetization of thin Ni(111) films¹⁸ we estimate the detection limit ($S/N \approx 1$) of our present setup as one-monolayer Ni at $T/T_c \approx 0.8$. This detection limit compares very favorably to the best available SMOKE data of ultrathin Ni

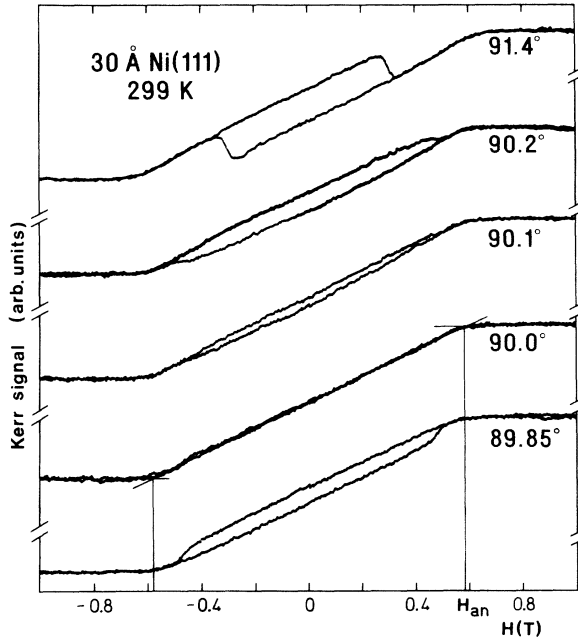


FIG. 4. Hard-axis magnetization loops of 30-Å Ni(111) as a function of the angle ϕ_h between the film plane and the applied field \mathbf{H} . Note the small changes in ϕ_h . At $\phi_h = 90^\circ$ one gets $H_{an} = 0.593 \pm 0.01$ T.

films.³ These authors obtain $S/N \approx 2.7$ for one-monolayer Ni/Ag(100) at $T/T_C \approx 0.63$ ($T_C \approx 175$ K).

In Fig. 3(b) the Kerr signal of the same film is measured with \mathbf{H} normal to the film ($\phi_h = 90^\circ$). The anisotropy field $H_{an} = 1.03$ T is determined in the usual way as the kink field of the perpendicular-magnetization curve.¹⁹ The Kerr signal of 30-Å Ni(111) on W(110) at room temperature is plotted in Fig. 4 ($\phi_h = 90^\circ$). We find $H_{an}(30 \text{ \AA}) = 0.63$ T in the same way. This represents the first quantitative *in situ* determination of H_{an} of ultrathin ferromagnetic films by the magneto-optic Kerr effect. The 30-Å value is reduced by almost 50% compared to 10 Å. This decrease is even larger if one takes into account that T/T_C of 30 Å is lower and should have a higher magnetocrystalline anisotropy (Table I). No hysteresis is observed as is expected for hard-axis loops. From H_{an} one obtains an effective anisotropy energy K_{eff} (Ref. 9) ac-

ording to

$$H_{an} = H_d + H_{cryst} = 4\pi(N_{\perp} - N_{\parallel})M(T) - \frac{2K_{eff}(T)}{M(T)}, \quad (1)$$

where we use the demagnetization factors $N_{\perp} = 1$, $N_{\parallel} = 0$ (Ref. 8) and the magnetization data $M(T)$ from Ref. 18. The effective anisotropy constants for our films are given in Table I. K_{eff} is negative, which means that the tendency of \mathbf{M} to lie in the film plane is favored. This tendency increases with decreasing thickness. The latter is caused by larger strains in the thinner samples due to the lattice mismatch of Ni(111) and W(110). In our case K_{eff} is related to the volume anisotropy energy of a hexagonal structure whose c axis is perpendicular to the film plane⁹

$$E_{an} = K_2 \sin^2 \theta + K_4 \sin^4 \theta + K_6^{\phi} \sin^6 \theta \cos 6\psi, \quad (2)$$

where θ is the angle between the magnetization and the c axis and ψ is the basal plane angle relative to the a axis. With this definition one obtains $K_2(T) = K_{eff}(T)$ (Ref. 20) in Eq. (1). The second-order anisotropy constant K_4 and the in-plane contribution K_6^{ϕ} cannot be determined in measurements at $\phi_h = 90^\circ$. Tilting the applied field by 0.1° away from the normal opens up the magnetization curve and hysteresis is observed. The characteristic change of this hysteresis as a function of ϕ_h (Fig. 4) shows the presence of an in-plane anisotropy.

To obtain an estimate for the magnitude of this in-plane anisotropy, we use the coercive fields H_c [Figs. 2 and 3(a)]. H_c is related to the in-plane anisotropy $K_6^{\phi}(T)$:¹⁹

$$H_c = \frac{2|K_6^{\phi}(T)|}{M(T)}. \quad (3)$$

To be precise Eq. (3) is correct only if the magnetization of the film switches as a single domain by coherent rotation. In the limit of ultrathin films with an in-plane magnetization single domain, formation upon remanently magnetizing the sample is very likely. This is supported by the experimental observation that freshly evaporated Co films (3–20 monolayers) form a single magnetic domain.²¹ Nevertheless the magnetization reversal of a single-domain film will occur by the nucleation and motion of domain walls. This lowers the experimentally determined H_c from the value given by Eq. (3). In the case of our fcc Ni films we find rather high coercive fields when compared to bulk Ni [$H_c \approx 10$ G (Ref. 19)]. We

TABLE I. Experimental results for Ni(111)/W(110): The anisotropy field H_{an} is determined as shown in Figs. 3(b) and 4. Magnetization data and Curie temperatures $T_C(d)$ are taken from Ref. 12 and 18. The in-plane anisotropy K_6^{ϕ} determined in Eq. (3) is negative. This is seen as follows: Our LEED data show that the a axis (Ref. 9) of our quasihexagonal fcc (111) film is parallel to W(100), the easy in-plane axis. This means that E_{an} (2) must be lowest at $\psi = 0^\circ$, $\theta = 90^\circ$ yielding a negative K_6^{ϕ} .

d Å	$T_C(d)$ K	$T/T_C(d)$	M G	H_c G	H_{an} kG	K_6^{ϕ} 10^4 erg/cm ³	K_{eff} 10^5 erg/cm ³
10	490	0.61	311	190	10.3	-2.95	-9.9
13	510	0.59	358	225	10	-4.03	-9.8
20	550	0.54	389	...	8.0	...	-6.1
25	583	0.51	413	130	6.30	-2.68	-2.3
30	588	0.51	430	151	5.93	-3.25	-1.1

take this as an indication that M rotates in a large domain and use Eq. (3) to determine $K_0^g(T)$. Interestingly, $K_0^g(T)$ values (Table I) calculated with the magnetization values given in Ref. 18 correspond reasonably well to the known anisotropy energy of bulk Ni ($\approx 4 \times 10^4$ erg/cm³). This leads us to use H_c as a lower estimate for the in-plane anisotropy $K_0^g(T)$ of Ni(111) films on W(110).

In conclusion we have presented an experimental setup to measure the magneto-optic Kerr effect in UHV in magnetic fields of up to 1.4 T. Large anisotropy fields of ul-

trathin Ni(111) films are determined *in situ* as a function of film thickness. The magnetocrystalline anisotropy energy of Ni(111) favors alignment in the plane along W(100) and increases with decreasing thickness.

We thank J. Kirschner for valuable information on the magneto-optic Kerr effect apparatus. Helpful discussions with B. Heinrich, D. Weller, C. M. Schneider, and U. Gradmann are acknowledged. This work was in support of in part by Deutsche Forschungsgemeinschaft, Sfb. 6.

*New address: Department of Material Science & Engineering, Stanford University, Stanford, CA 94305-2205.

¹C. Liu, E. R. Moog, and S. D. Bader, Phys. Rev. Lett. **60**, 2422 (1988).

²J. Araya-Pochet, C. A. Ballentine, and J. L. Erskine, Phys. Rev. B **38**, 7846 (1988).

³C. A. Ballentine, R. L. Fink, J. Araya-Pochet, and J. L. Erskine, Appl. Phys. A **49**, 459 (1989).

⁴C. Liu and S. D. Bader, in *Magnetic Properties of Low-Dimensional Systems II*, edited by L. M. Falicov, F. Mejia-Lira, and Y. L. Moran-Lopez, Springer Proceedings in Physics Vol. 50 (Springer-Verlag, Berlin, 1990), p. 61.

⁵C. M. Schneider, P. Bressler, P. Schuster, J. Kirschner, J. J. de Miguel, and R. Miranda, Phys. Rev. Lett. **64**, 1059 (1990).

⁶J. W. D. Martens, W. L. Peters, P. Q. J. Nederpel, and M. Ermann, J. Appl. Phys. **55**, 1100 (1984).

⁷F. Schmidt and A. Hubert, J. Magn. Magn. Mater. **61**, 307 (1986).

⁸M. Farle, A. Berghaus, and K. Baberschke, Phys. Rev. B **39**, 4838 (1989).

⁹B. Coqblin, *The Electronic Structure of Rare-Earth Metals and Alloys: the Magnetic Heavy Rare-Earths* (Academic, London, 1977).

¹⁰U. Gradmann, J. Magn. Magn. Mater. **54-57**, 733 (1986).

¹¹K. Baberschke, M. Zomack, and M. Farle, in *Magnetic Prop-*

erties of Low-Dimensional Systems, edited by L. M. Falicov and Y. L. Moran-Lopez, Springer Proceedings in Physics Vol. 14 (Springer-Verlag, Berlin, 1986), p. 84.

¹²Yi Li, M. Farle, and K. Baberschke, Phys. Rev. B **41**, 9596 (1990).

¹³D. Mauri, D. Scholl, H. C. Siegmann, and E. Kay, Appl. Phys. A **49**, 439 (1989).

¹⁴K. Bethke, Diplomarbeit, Rheinisch-Westfälische Technische Hochschule Aachen, 1988 (unpublished).

¹⁵G. Metzger, P. Pluvinage, and R. Torguet, Ann. Phys. (Paris) **10**, 5 (1965).

¹⁶E. R. Moog, C. Liu, S. D. Bader, and J. Zak, Phys. Rev. B **39**, 6949 (1989).

¹⁷U. Stetter, M. Farle, and K. Baberschke, Verh. Dtsch. Phys. Ges. **4**, 924 (1990).

¹⁸R. Bergholz and U. Gradmann, J. Magn. Magn. Mater. **45**, 389 (1984).

¹⁹S. V. Vonsovskii, *Magnetism* (Wiley, New York, 1974), Vol. 2, p. 1014ff.

²⁰A. Berghaus, M. Farle, Yi Li, and K. Baberschke, *Magnetic Properties of Low-Dimensional Systems II* (Ref. 4), p. 61.

²¹H. P. Oepen, M. Benning, C. M. Schneider, and J. Kirschner, Vacuum (to be published); and C. M. Schneider (private communication).